



Short communication

Electrochemical properties of $\text{Li}_{1.4}\text{Al}_{0.4}\text{Ti}_{1.6}(\text{PO}_4)_3$ synthesized by a co-precipitation method

Lezhi Huang, Zhaoyin Wen*, Meifen Wu, Xiangwei Wu, Yu Liu, Xiuyan Wang

CAS Key Laboratory of Materials for Energy Conversion, Shanghai Institute of Ceramics, Chinese Academy of Sciences, No. 1295 Dingxi Road, Shanghai 200050, PR China

ARTICLE INFO

Article history:

Received 14 September 2010

Received in revised form

15 November 2010

Accepted 25 November 2010

Available online 2 December 2010

Keywords:

Lithium ion electrolyte

All-solid-state lithium battery

Co-precipitation

Conductivity

ABSTRACT

Sub-micron $\text{Li}_{1.4}\text{Al}_{0.4}\text{Ti}_{1.6}(\text{PO}_4)_3$ (LATP) ceramic powder is synthesized by a co-precipitation method which can be applied for mass production. A pure Nasicon phase is confirmed by X-ray diffraction analysis and the primary particle size of the product is 200–500 nm. The sinterability of LATP is investigated and the relative density of 97% reached at a sintering temperature as low as 900 °C for 6 h. The bulk lithium ionic conductivity of the sintered pellet is $2.19 \times 10^{-3} \text{ S cm}^{-1}$, and a total conductivity of $1.83 \times 10^{-4} \text{ S cm}^{-1}$ is obtained.

© 2010 Elsevier B.V. All rights reserved.

1. Introduction

Safety is one of the main factors limiting the large scale application of lithium batteries. Due to the organic liquid electrolytes currently used in commercial lithium batteries are flammable, the short-circuit of the batteries may lead to fire or even exploding [1]. All-solid-state lithium batteries are of high safety and stability because the electrolytes have high melting point and are unpenetrable [1]. Inorganic type electrolytes, such as Li_3N [2], $\text{Li}_x\text{La}_{1-x}\text{TiO}_3$ [3], NASICON (sodium super ionic conductor) structure phosphates $\text{Li}_{1+x}\text{M}'_x\text{M}''_{2-x}(\text{PO}_4)_3$ ($\text{M}' = \text{Al, Y, Fe etc.}; \text{M}'' = \text{Ti, Ge, Hf etc.}$) [4–9] and so on, are considered as possible electrolyte candidates for all-solid-state lithium batteries.

NASICON structured ceramics are among the most promising candidates for all-solid-state electrolytes because of their high conductivity at room temperature and high melting point. Aono et al. reported a maximum bulk conductivity of $10^{-3} \text{ S cm}^{-1}$ at 300 K and $x = 0.3$ for $\text{Li}_{1+x}\text{Al}_x\text{Ti}_{2-x}(\text{PO}_4)_3$ [10]. This almost can meet the requirements of practical lithium batteries. Weppner et al. have prepared an all-solid-state battery of $\text{Li}_4\text{Ti}_5\text{O}_{12}/\text{Li}_{1.3}\text{Al}_{0.3}\text{Ti}_{1.7}(\text{PO}_4)_3/\text{LiMn}_2\text{O}_4$ operated at room temperature [11].

One of the problems of NASICON structured electrolyte for practical applications is the difficulty in mass production. This type of ceramic electrolytes has been synthesized by various techniques,

such as solid state reaction, sol–gel process and melting–quenching method [12–15]. All of the above synthetic methods cannot be easily applied to the mass production due to high energy consumption and impurities in the final production.

In this work, a chemical synthesis route suitable for mass production based on a co-precipitation method for the sub-micron $\text{Li}_{1+x}\text{Al}_x\text{Ti}_{2-x}(\text{PO}_4)_3$ ($x = 0.4$) (LATP) was developed. The sinterability of the as-prepared powders was studied. AC impedance was measured and the conductivity of the ceramics at room temperature was therefore obtained.

2. Experimental

All reagents were of analytical grade purity. $\text{Li}_2\text{C}_2\text{O}_4$ and $\text{Al}(\text{NO}_3)_3 \cdot 9\text{H}_2\text{O}$ were dissolved by deionized water and added dropwise into excessive NH_4HCO_3 solution under vigorous stirring to generate the precipitates. To avoid the evaporation of lithium during synthesis and sintering, 10% excessive amount of $\text{Li}_2\text{C}_2\text{O}_4$ was added in the precursors. $\text{Ti}(\text{OC}_4\text{H}_9)_4$ and $\text{NH}_4\text{H}_2\text{PO}_4$ were dropped into the solution afterwards and the stirring was kept for 2 h. All the above processes were preceded at 80 °C in a water bath. The mixture was dried at 120 °C to vaporize the solvent. The remained powder was pyrolyzed at 350 °C for 2 h and then calcined at 800 °C for 30 min. The as-prepared powder was ground by ball-milling and pelletized by isostatic press at 200 MPa. The pellets were sintered at different temperatures to investigate their sinterability.

X-ray diffraction (XRD) was carried out to analyze the crystal structure of the products. The morphology was recorded on a JSM-6700F scanning electronic microscope (SEM). The AC impedance

* Corresponding author. Tel.: +86 21 52411704; fax: +86 21 52413903.

E-mail addresses: zywen@mail.sic.ac.cn, liangxiao@student.sic.ac.cn (Z. Wen).

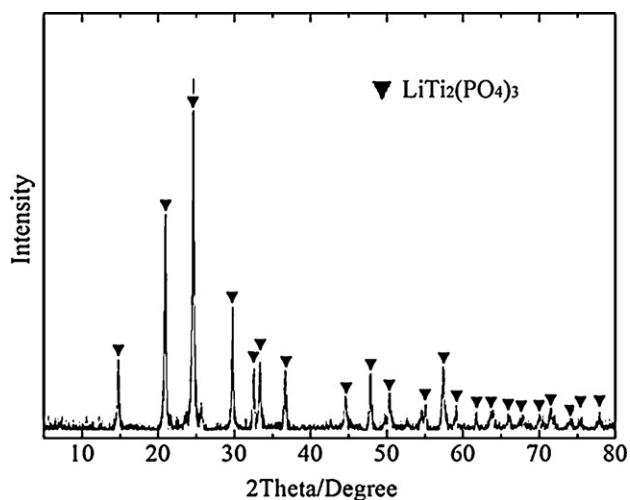


Fig. 1. XRD patterns of the powder product.

was tested on an AUTOLAB electrochemical workstation from 1 MHz to 0.01 Hz with gold layers at both sides as the blocking electrodes.

3. Results and discussion

3.1. Material preparation

Fig. 1 shows XRD patterns of the as-prepared powders. A pure NASICON phase is indicated. The lattice constants calculated from XRD data are $a = 0.84716$ nm and $c = 2.07644$ nm, which belong to $R\bar{3}c$ space group. The crystal lattice of the obtained products showed a slightly shrinkage compared to the standard data of $\text{LiTi}_2(\text{PO}_4)_3$, which were $a = 0.8513$ nm and $c = 20.878$ nm (JCPDF card No. 00-35-0754). This was mainly attributed to the partially substitution of Ti in the lattice of $\text{LiTi}_2(\text{PO}_4)_3$ by Al, which has a smaller atomic diameter. Synthesis of LATP by a solid-state reaction may bring impurities like AlPO_4 due to the reaction of Al^{3+} and PO_4^{3-} [16]. As demonstrated in this study, high purity of NASICON phase can be obtained by the co-precipitation method.

Fig. 2 shows the morphology of the as-prepared powder. The primary particles are mainly in sub-micron range of 200–500 nm. This small particle size can afford the ceramic powder good sin-

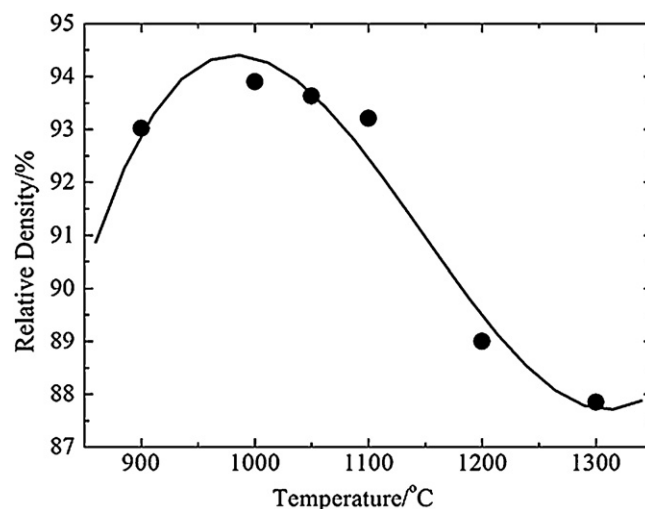


Fig. 3. Relative density of LATP pellets after sintering.

tering behavior. However, some agglomerates were observed. It was considered to be the consequence of the characteristic of carbonate precipitation. Ball milling using ZrO_2 balls and alcohol as solvent was introduced to reduce the agglomerations. EDS analysis showed that no impurity elements were introduced into the product. Some particles were mainly in the range of 0.1–1 μm by grinding the powder for 10 h. However, part of the agglomerations cannot be reduced into primary particle size by a simple grinding.

3.2. Sinterability

3.2.1. Sintering temperature

The ground powder was pressed into pellets with a relative density nearly 60% by isostatic pressing at 200 MPa. The pellets were sintered at different temperatures for 3 h. The relative densities of the sintered pellets were given and compared in Fig. 3. As seen, the relative density reached 93.90% at 1000 $^\circ\text{C}$, and 93.02%, 93.63% and 93.21% at 900 $^\circ\text{C}$, 1050 $^\circ\text{C}$ and 1100 $^\circ\text{C}$, respectively. The relative densities declined sharply at 1200 $^\circ\text{C}$ and 1300 $^\circ\text{C}$ reaching to below 90%, which could be ascribed to the loss of lithium in the LATP at high temperature.

As seen in Fig. 4, all the sintered samples presented characteristic diffraction peak of aluminum phosphate phase at about $2\theta = 22^\circ$.

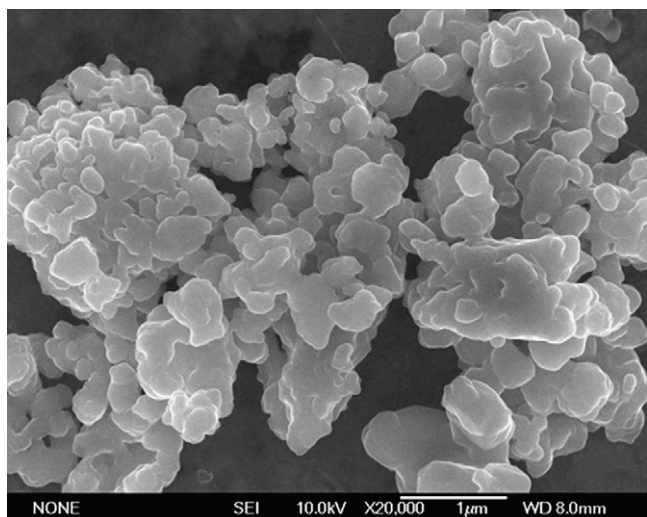


Fig. 2. Morphology of the LATP powder.

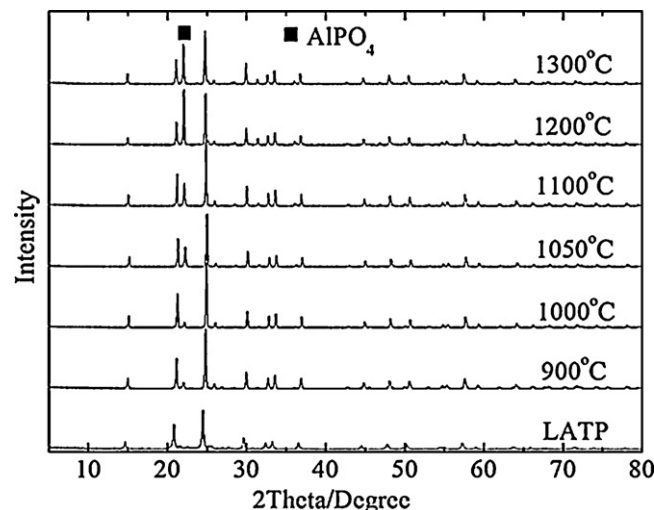


Fig. 4. XRD patterns of the sintered pellets.

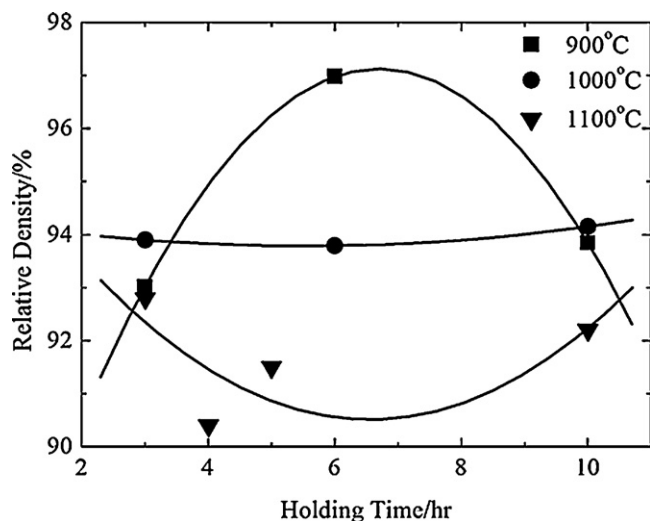


Fig. 5. Relative density of LATP pellets vs. holding time.

The peak intensity of the impurity phase increased with the sintering temperature, indicating that the lithium evaporation was more serious at higher temperature. An obvious increase of the peak intensity corresponding to AlPO_4 could be observed in the sample sintered at 1200°C and 1300°C . It well accorded with the relative density obtained.

Based on the results, it was concluded that a relatively low temperature, e.g., 900°C or 1000°C , would be suitable for sintering the LATP ceramics.

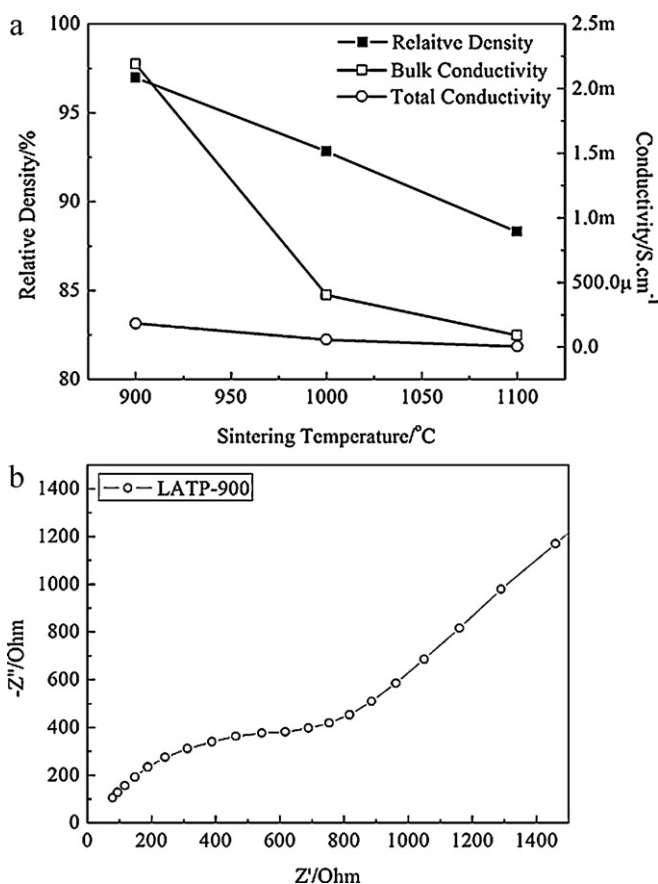


Fig. 6. (a) Relative density and conductivity of LATP samples sintered at different temperatures. (b) AC impedance spectra of LATP ceramic electrolyte sintered at 900°C for 6 h.

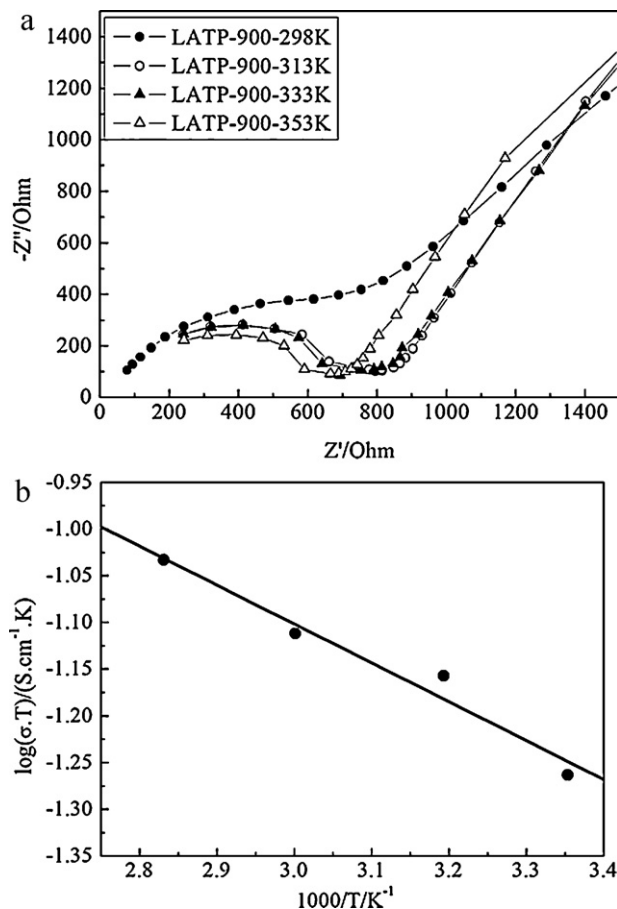


Fig. 7. (a) AC impedance spectrum at 298–353 K of the LATP ceramic electrolyte sintered at 900°C for 6 h. (b) Arrhenius curve of LATP ceramic electrolyte sintered at 900°C for 6 h.

3.2.2. Holding time

Fig. 5 shows the effect of holding time on the relative density of LATP pellets at 900, 1000 and 1100°C , respectively. Increase of the holding time at 900°C increased the relative density. A relative density of 97% was reached for the sample sintered at 900°C for 6 h. However, the relative density of the sample did not further increase as the holding time was over 6 h. No obvious effect of holding time on the densification was observed as the sintering temperature was higher than 900°C .

3.3. Conductivity measurement

The conductivity of the LATP pellets sintered at 800 – 1100°C for 6 h was measured by AC impedance at room temperature with gold at both sides as the blocking electrode. The result presented a characteristic capacitance circuit as shown in Fig. 6. The relationship between conductivity and relative density was shown in Fig. 6(a). The first intersection of the semi-circle corresponds to the bulk resistance and the later one corresponds to the total resistance. Obviously, the conductivity greatly depended on the relative density of the ceramics. The sample sintered at 900°C , which had the highest density showed the best conductivity at room temperature.

The conductivity measurement results for the LATP-900 sample were shown in Fig. 6(b). The semi-circle corresponded to the lithium ion transportation in the ceramic electrolyte. The straight line appeared afterward was caused by the lithium ion diffusion in the electrode. The conductivity of the ceramic electrolyte was calculated as $2.19 \times 10^{-3} \text{ S cm}^{-1}$ for bulk and $1.83 \times 10^{-4} \text{ S cm}^{-1}$ for total conductivity. It was noticeable that the total conductivity was

more than one order of magnitude lower than the bulk conductivity. Anyway, the LATP ceramics showed an acceptable conductivity of lithium ion at room temperature.

Fig. 7 shows the AC impedance of LATP-900 tested in the range of 289–353 K. The relationship between conductivity and temperature well fit to the Arrhenius equation as $\log(\sigma T) = A - E_a/RT$, in which E_a represents the activation energy of the ceramic electrolyte. The E_a of LATP-900 sample calculated from the slope of linear fitted line was 0.35 eV. For typical NASICON structured lithium electrolyte, the E_a of crystal bulk is constant at about 0.3 eV. But the E_a of grain boundary may vary with the substitutional amount of M^{4+} by M^{3+} due to the structural change and the degree of densification [1]. The substitution of Ti^{4+} by Al^{3+} might decrease the E_a of the grain boundary greatly [17].

4. Conclusion

In this work, co-precipitation method was adopted to produce pure phase LATP powder. This method is applicable for mass production. The sinterability of the as-prepared LATP was optimized. The maximum relative density reached 97% for the sample sintered at 900 °C for 6 h. The LATP electrolyte showed an acceptable conductivity at room temperature, which was $2.19 \times 10^{-3} \text{ S cm}^{-1}$ for bulk, and $1.83 \times 10^{-4} \text{ S cm}^{-1}$ for total conductivity.

Acknowledgements

This work was financially supported by Natural Science Foundation of China (NSFC, Project Nos. 50973127 and 50672114), 973 Project of China No. 2007CB209700, as well as Research Projects from the Science and Technology Commission of Shanghai Municipality No. 08DZ2210900.

References

- [1] G. Adachi, N. Imanaka, H. Aono, *Adv. Mater.* 8 (1996) 127–135.
- [2] U.V. Alpen, *J. Solid State Chem.* 29 (1979) 379–392.
- [3] K. Yang, J. Wang, K. Fung, *J. Alloys Compd.* 458 (2008) 415–424.
- [4] H. Aono, E. Sugimoto, Y. Sadaoka, *Solid State Ionics* 40/41 (1990) 38–42.
- [5] H. Aono, E. Sugimoto, Y. Sadaoka, *J. Electrochem. Soc.* 137 (1990) 1023–1027.
- [6] C.J. Leo, B.V.R. Chowdari, G.V. Subba Rao, *Mater. Res. Bull.* 37 (2002) 1419–1430.
- [7] E.R. Losilla, S. Bruque, M.A.G. Aranda, *Solid State Ionics* 112 (1998) 53–62.
- [8] C.M. Chang, S.H. Hong, H.M. Park, *Solid State Ionics* 176 (2005) 2583–2587.
- [9] P. Maldonado-Manso, E.R. Losilla, M. Matinez-Lara, *Chem. Mater.* 15 (2003) 1879–1885.
- [10] H. Aono, E. Sugimoto, Y. Sadaoka, *J. Electrochem. Soc.* 136 (1989) 590–591.
- [11] P. Birke, F. Salam, S. Doring, *Solid State Ionics* 118 (1999) 149–157.
- [12] X. Xu, Z. Wen, J. Wu, *Solid State Ionics* 178 (2007) 29–34.
- [13] X. Xu, Z. Wen, X. Yang, *Mater. Res. Bull.* 43 (2008) 2334–2341.
- [14] K. Takeda, K. Fujimoto, T. Inada, *Appl. Surf. Sci.* 189 (2002) 300–306.
- [15] J. Wolfenstine, D. Foster, J. Read, *J. Power Sources* 182 (2008) 626–629.
- [16] K. Arbi, S. Mandal, J.M. Rojo, *Chem. Mater.* 14 (2002) 1091–1097.
- [17] H. Aono, E. Sugimoto, Y. Sadaoka, *Chem. Lett.* 19 (1990) 1825.